

1 Paradoxical phase response of gamma rhythms facilitates their
2 entrainment in heterogeneous networks

3 Xize Xu, Hermann Riecke

4 November 17, 2020

5 Department of Engineering Science and Applied Mathematics, Northwestern University, Evanston, IL
6 60208, USA

Abstract

The synchronization of different γ -rhythms arising in different brain areas has been implicated in various cognitive functions. Here, we focus on the effect of the ubiquitous neuronal heterogeneity on the synchronization of PING (pyramidal-interneuronal network gamma) and ING (interneuronal network gamma) rhythms. The synchronization properties of rhythms depends on the response of their collective phase to external input. We therefore determined the macroscopic phase-response curve for finite-amplitude perturbations (fmPRC), using numerical simulation of all-to-all coupled networks of integrate-and-fire (IF) neurons exhibiting either PING or ING rhythms. We show that the intrinsic neuronal heterogeneity can qualitatively modify the fmPRC. While the phase-response curve for the individual IF-neurons is strictly positive (type I), the fmPRC can be biphasic and exhibit both signs (type II). Thus, for PING rhythms, an external excitation to the excitatory cells can, in fact, delay the collective oscillation of the network, even though the same excitation would lead to an advance when applied to uncoupled neurons. This paradoxical delay arises when the external excitation modifies the internal dynamics of the network by causing additional spikes of inhibitory neurons, whose delaying within-network inhibition outweighs the immediate advance caused by the external excitation. These results explain how intrinsic heterogeneity allows the PING rhythm to become synchronized with a periodic forcing or another PING rhythm for a wider range in the mismatch of their frequencies. We demonstrate a similar mechanism for the synchronization of ING rhythms. Our results identify a potential function of neuronal heterogeneity in the synchronization of coupled γ -rhythms, which may play a role in neural information transfer via communication through coherence.

Author Summary

The interaction of a large number of oscillating units can lead to the emergence of a collective, macroscopic oscillation in which many units oscillate in near-unison or near-synchrony. This has been exploited technologically, e.g., to combine many coherently interacting, individual lasers to form a single powerful laser. Collective oscillations are also important in biology. For instance, the circadian rhythm of animals is controlled by the near-synchronous dynamics of a large number of individually oscillating cells. In animals and humans brain rhythms reflect the coherent dynamics of a large number of neurons and are surmised to play an important role in the communication between different brain areas. To be functionally relevant, these rhythms have to respond to external inputs and have to be able to synchronize with each other. We show that the ubiquitous heterogeneity in the properties of the individual neurons in a network can contribute to that ability. It can allow the external inputs to modify the internal network dynamics such that the network can follow these inputs over a wider

40 range of frequencies. Paradoxically, while an external perturbation may delay individual neurons, their
41 ensuing within-network interaction can overcompensate this delay, leading to an overall advance of the
42 rhythm.

43 1 Introduction

44 Collective oscillations or rhythms representing the coherent dynamics of a large number of coupled
45 oscillators play a significant role in many systems. In the technological realm they range from laser
46 arrays and Josephson junctions to micromechanical oscillators [1, 2]. Among the important biological
47 examples are the heart rhythm, the circadian rhythm generated by the suprachiasmatic nucleus [3],
48 the segmentation clock controlling the somite formation during development [4], and brain waves [5].
49 One prominent brain rhythm is the widely observed γ -rhythm with frequencies in the range 30-100Hz.
50 The coherent spiking of the neurons underlying this rhythm likely enhances the downstream impact
51 of the neurons participating in the rhythm. The rhythmic alternation of low and high activity has
52 been suggested to play a significant role in the communication between different brain areas [6, 7].
53 That communication has also been proposed to be controlled by the coherence of the rhythms in the
54 participating brain areas [8–13].

55 For collective oscillations or rhythms to play a constructive role in a system they need to respond
56 adequately to external perturbations and stimuli. For instance, for the circadian rhythm it is essential
57 that it can be reliably entrained by light and phase-lock to its daily variation. Similarly, if rhythms are
58 to play a significant role in the communication between different brain areas, their response to input
59 from other areas represents a significant determinant of their function. Moreover, the stimulation and
60 entrainment of γ -rhythms by periodic sensory input is being considered as a therapeutic approach for
61 some neurodegenerative diseases [14].

62 Even small perturbations can affect oscillations significantly in that they can advance or delay the
63 oscillations, i.e. they can change the phase of the oscillators. This change typically depends not
64 only on the strength of the perturbation but, importantly, also on the timing of the perturbations
65 and is expressed in terms of the phase response curve (PRC), which has been studied extensively for
66 individual oscillators [15]. For infinitesimal perturbations the PRC can be determined elegantly using
67 the adjoint method [16].

68 If the collective oscillation of a network of interacting oscillators is sufficiently coherent, that system

69 can be thought of as a single effective oscillator. Consequently, the response of the macroscopic
70 phase of the collective oscillation to external perturbations and the mutual interaction of multiple
71 collective oscillations is of interest. The macroscopic phase-response curve (mPRC) has been obtained
72 in various configurations, including noise-less heterogeneous phase oscillators [17, 18], noisy identical
73 phase oscillators [19, 20], noisy excitable elements [21], and noisy oscillators described by the theta-
74 model [22], which is equivalent to the quadratic integrate-fire model for spiking neurons. Recent
75 work has used the reduction of networks of quadratic integrate-fire neurons to two coupled differential
76 equations for the firing rate and the mean voltage [23], which is related to the Ott-Antonsen theory
77 [24, 25], to develop a method to obtain the infinitesimal macroscopic PRC (imPRC) for excitatory-
78 inhibitory spiking networks [26, 27].

79 A key difference between the response of an individual oscillator to a perturbation and that of a
80 collective oscillation is the fact that the degree of synchrony of the collective oscillation can change
81 as a result of the perturbation, reflecting a change in the relations between the individual oscillators.
82 Thus, the phase response of a collective oscillation to a brief perturbation consists not only of the
83 immediate change in the phases of the individual oscillators caused by the perturbation, but includes
84 also a change in the collective phase that can result from the subsequent convergence back to the
85 phase relationship between the oscillators corresponding to the synchronized state, which is likely to
86 have been changed by the perturbation [18]. Interestingly, it has been observed that the infinitesimal
87 macroscopic phase response can be qualitatively different from the phase response of the individual
88 elements. Thus, even if the individual oscillators have a type-I PRC, i.e. a PRC that is strictly positive
89 or negative, the mPRC of the collective oscillation can be of type II, i.e. it can exhibit a sign change
90 as a function of the phase [21, 22, 28].

91 Here we investigate the interplay between external perturbations and the internal interactions among
92 neurons in inhibitory and in excitatory-inhibitory networks exhibiting γ -rhythms of the ING- and
93 of the PING-type. We focus on networks comprised of neurons that are not identical, leading to a
94 spread in their individual phases and a reduction in the degree of their synchrony. How does this
95 phase dispersion affect the response of the macroscopic phase of the rhythm to perturbations? Does
96 it modify the ability of the network to follow a periodic perturbation ?

97 We show that the dispersion in the phase together with the within-network interactions among the
98 neurons can be the cause of a paradoxical phase response: an external perturbation that *delays* each
99 individual neuron can *advance* the macroscopic rhythm. We identify the following mechanism under-

100 lying this paradoxical response: external perturbations that delay individual neurons sufficiently allow
101 the within-network inhibition generated by early-spiking neurons to suppress the spiking of less excited
102 neurons. This results in a reduced within-network inhibition, which reduces the time to the next spike
103 volley, speeding up the rhythm. This paradoxical phase response increases with the neuronal hetero-
104 geneity and allows the network to phase-lock to periodic external perturbations over a wider range of
105 detuning. Thus, the desynchronization within the network enhances its synchronizability with other
106 networks. The mechanism is closely related to that underlying the enhancement of synchronization of
107 collective oscillations by uncorrelated noise [29] and the enhanced entrainment of the rhythm of a ho-
108 mogeneous network to periodic input if that input exhibits phase dispersion across the network [30,31].
109 We demonstrate and analyze these behaviors for networks of inhibitory neurons (ING-rhythm) and for
110 networks comprised of excitatory and inhibitory neurons (PING-rhythm).

111 2 Results

112 We investigated the impact of neuronal heterogeneity on the response of the phase of γ -rhythms to
113 brief external perturbations and the resulting ability of rhythms to synchronize to periodic input.
114 As described in the Methods, we used networks comprised of minimal integrate-fire neurons that in-
115 teract with each other through synaptic pulses modeled via delayed double-exponentials. To study
116 ING-rhythms all neurons were inhibitory, while for the PING-rhythms we used excitatory-inhibitory
117 networks. In both cases, the coupling within each population was all-to-all. Throughout, we imple-
118 mented the neuronal heterogeneity by injecting a different steady bias current I_{bias} into each neuron.
119 Our analysis suggests that the origin of the neuronal heterogeneity plays only a minor role as long as
120 it leads to a dispersion of their spike times [29].

121 Paradoxical Phase Response of Heterogeneous Networks: ING-Rhythm

122 In the absence of external perturbations the all-to-all inhibition among the neurons lead to rhythmic
123 firing of the neurons. Due to their heterogeneity they did not spike synchronously but sequentially, as
124 shown in Fig.1A, where the neurons are ordered by the strength of their bias current. The dependence
125 of the phase dispersion on the coefficient of variation of the heterogeneity in the bias current (CV)
126 is shown in Suppl. Figure S1. For sufficiently large heterogeneity some neurons never spiked: while
127 the weak bias current they received would have been sufficient to induce a spike eventually, the strong

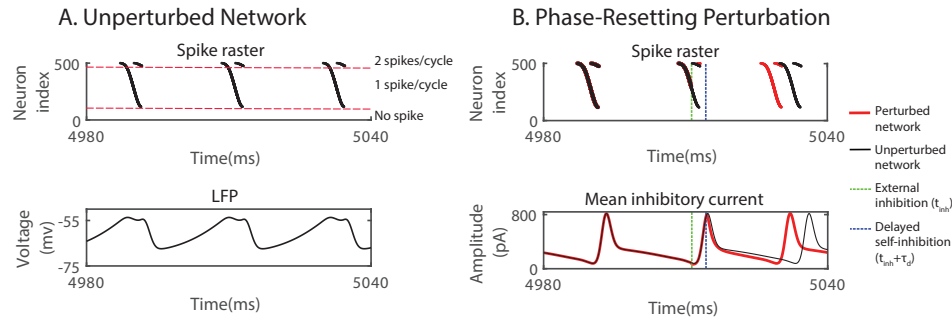


Figure 1: ING-rhythm can be advanced by inhibition while individual neurons are delayed.

(A) Top: spike raster of neurons spiking sequentially in the order of their input strength (increasing with neuron index). Bottom: mean voltage across the network (LFP). (B) External inhibition advanced the rhythm. Top: raster plot of spikes without (black) and with (red) external inhibitory pulse. Bottom: Average of the total inhibitory current each neuron received from the other neurons within the network.

$I^{(I)} = 20.4$ pA, $C_V^{(I)} = 0.15$, $f_{network} = 47$ Hz. In (B), perturbations were made with a square-wave inhibitory current pulse with duration 0.1 ms and amplitude 3200 pA to each neuron, resulting in a 4 mV rapid hyperpolarization.

128 inhibition that was generated by the neurons spiking earlier in the cycle suppressed those late spikes.

129 Neurons with strong bias current could spike multiple times.

130 A brief, inhibitory external input delivered to all neurons (green dashed line in Fig.1B) delayed each
131 neuron. The degree of this individual delay depended on the timing of the input, as is reflected
132 in the PRC of the individual neurons. If the perturbation was applied during the time between the
133 spike volleys, the delay of each neuron had no further consequence and the overall rhythm was delayed.

134 However, if the same inhibitory perturbation arrived during a spike volley (dashed green line in Fig.1B),
135 it could advance the overall rhythm. As illustrated in Fig.1B, only the spiking of the late neurons was
136 delayed by the perturbation. Importantly, with this delay some neurons did not spike before the
137 within-network inhibition triggered by the early-spiking neurons (dashed blue line in Fig.1B) became
138 strong enough to suppress the spiking of the late neurons altogether. With fewer neurons spiking, the
139 all-to-all inhibition within the network was reduced, allowing all neurons to recover earlier, which lead
140 to a shorter time to the next spike volley. If the speed-up was larger than the immediate delay induced
141 by the external inhibition, the overall phase of the rhythm was advanced by the delaying inhibition.

142 As the example in Fig.1B shows, the paradoxical phase response requires proper timing of the per-
143 turbation. We therefore determined quantitatively the macroscopic phase-response curve (PRC) of
144 the rhythm. To do so we measured computationally the amount a brief current injection shifted the
145 phase of the rhythm (Fig.2A). We defined the phase as the normalized time since the first spike in

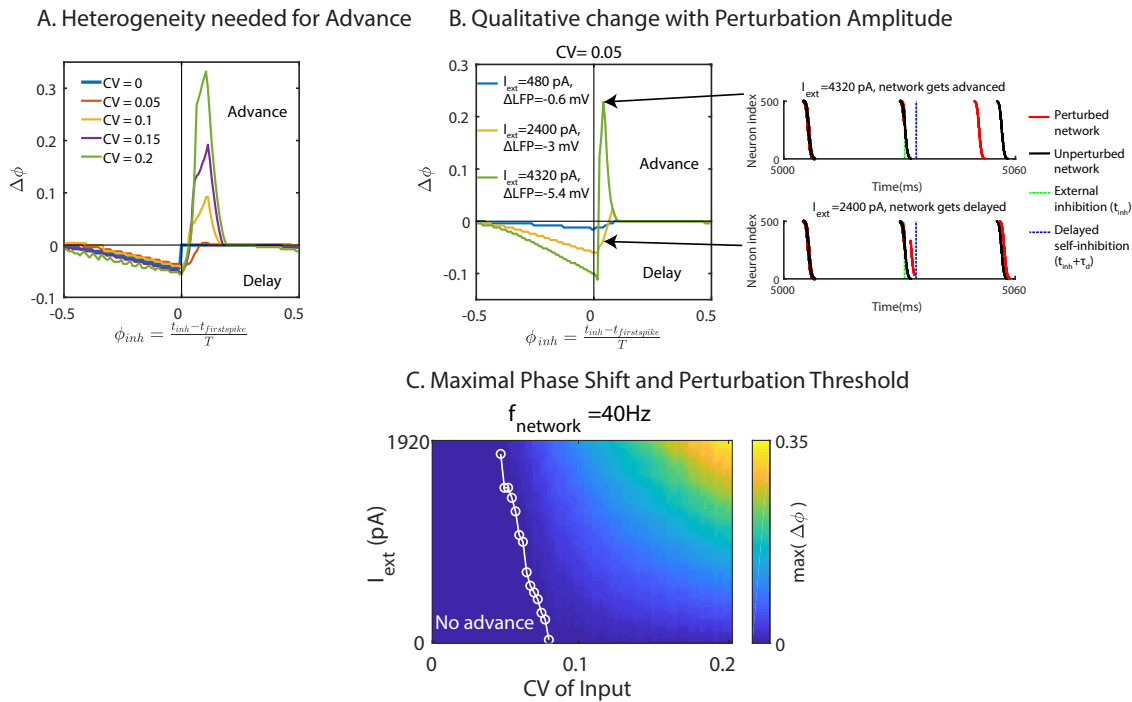


Figure 2: fmPRC of heterogeneous ING network. (A) Phase shift in response to inhibition for different neuronal heterogeneity but fixed natural frequency ($f_{network} = 40\text{Hz}$). The paradoxical phase advance increased with neuronal heterogeneity. (B) fmPRC changed qualitatively with the amplitude of the perturbation. Left: fmPRC for three different perturbation amplitudes. Right: raster plot of spikes without (black) and with (red) external inhibition. Top: strong perturbation advanced the network. Bottom: weak perturbation applied at the same time as in the top figure. The network was delayed. (C) Maximal phase advance as a function of neuronal heterogeneity and external inhibition strength. The threshold of the inhibition amplitude to obtain an advance decreased with heterogeneity (white line). $f_{network}$ was kept constant ($f_{network} = 40\text{Hz}$). In (A)-(C), perturbations were made with a square-wave inhibitory current pulse with duration 0.1 ms to each interneuron. In (A), the amplitude of the current was 1600 pA, resulting in a 2 mV rapid hyperpolarization.

146 the most recent volley of spikes. Reflecting the strictly positive PRC of the individual integrate-fire
147 neurons, without heterogeneity ($CV = 0$) external inhibition always delayed the rhythm, independent
148 of the timing of the pulse. In contrast, in heterogeneous networks the rhythm could be advanced if the
149 same inhibitory perturbation was applied shortly after the first spikes in the spike volley ($\phi_{inh} > 0$).
150 Increasing the neuronal heterogeneity enhanced this phase advance, since it shifted the within-network
151 inhibition driven by the leading neurons to earlier times, while it delayed the lagging neurons. As a
152 result, for the same external perturbation, a larger fraction of neurons that would spike in the absence
153 of the external inhibition was sufficiently delayed to have their spikes be suppressed by the within-
154 network inhibition (cf. Fig.1B), reducing the within-network inhibition and with it the time to the
155 next spike volley. To keep the frequency of the unperturbed network fixed in Fig.2A, we reduced the
156 tonic input with increasing heterogeneity, which enhanced the phase advance. However, even if the
157 tonic input was kept fixed, the phase advance increased with heterogeneity (Suppl. Fig.S2).

158 For weak heterogeneity the paradoxical phase response occurred only for sufficiently strong perturba-
159 tions, i.e. it did not arise in the infinitesimal macroscopic PRC (imPRC). Thus, the phase response
160 changed qualitatively as the amplitude of the perturbation was strong enough to delay the spikes of
161 sufficiently many slow neurons until the self-inhibition of the network set in and suppressed their spikes
162 (Fig.2B). As the CV of the neurons was increased, the dispersion was large enough that the spikes
163 of the lagging neurons were suppressed by the self-inhibition of the network even in the absence of
164 an external perturbation. Above that threshold value of CV the paradoxical phase response occurred
165 even for infinitesimal perturbations (Fig.2C).

166 The paradoxical phase response was robust with respect to changes in the natural frequency of the
167 network, the coupling strength, and the effective synaptic delay, as long as the rhythm persisted.
168 The paradoxical phase advance increased with decreasing natural frequency of the network, since
169 the inhibition had a stronger effect for lower mean input strength (Fig.3A). Changing the within-
170 network coupling strength by a factor of 2 up or down did not substantially affect the paradoxical
171 phase response (Fig.3B) nor the strength of the rhythm (Fig.3C). Even without explicit synaptic delay
172 ($\tau_d = 0$), the effective delay given by the double-exponential synaptic interaction was sufficient to render
173 a paradoxical response (Fig.3D). However, when this effective delay was reduced by decreasing the
174 rise time τ_1^I of the synaptic current, the rhythm itself developed a strong subharmonic component and
175 eventually disintegrated (Fig.3E). In the subharmonic regime the paradoxical phase advance alternated
176 in consecutive cycles of the rhythm.

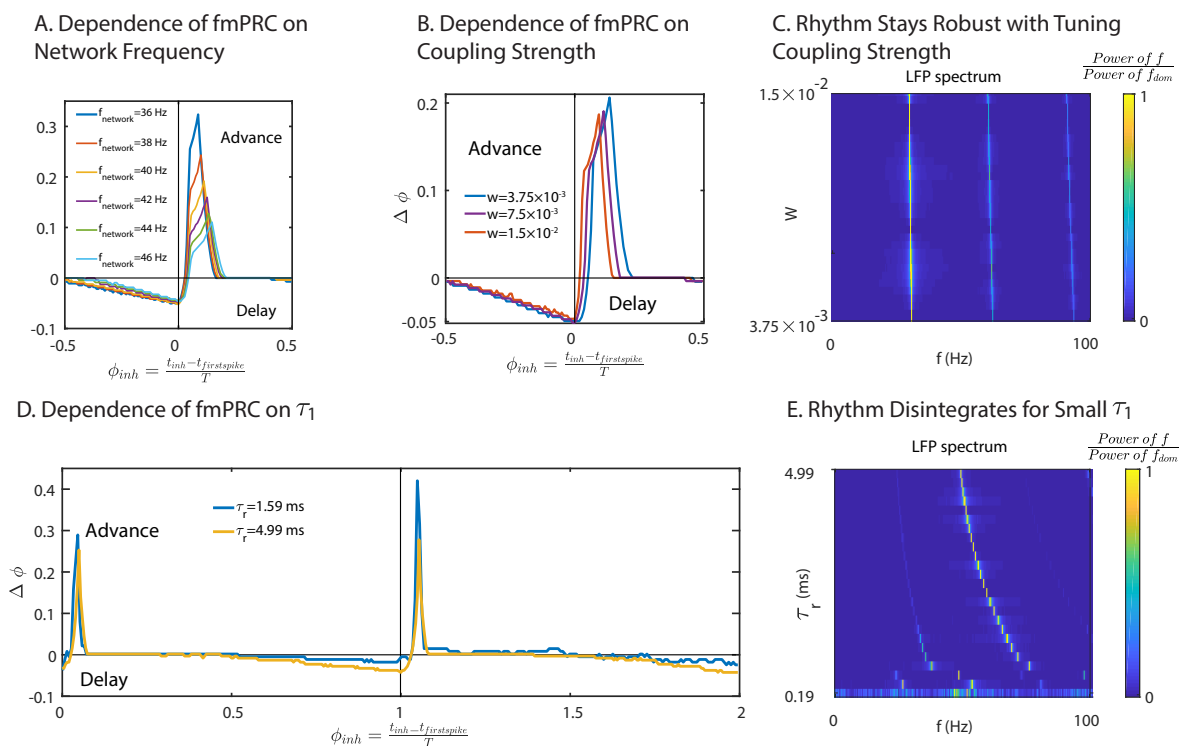


Figure 3: The paradoxical phase response of a heterogeneous ING network is robust. (A) The phase advance of the fmPRC decreased with the natural frequency ($CV(I) = 0.15$). (B) The fmPRC did not depend sensitively on the within-network coupling strength W ($CV(I) = 0.15$, $I(I) = 15.8$ pA). (C) The Fourier spectrum of the LFP as a function of the coupling strength W . Parameters as in (B). (D) Paradoxical phase response in the absence of an explicit delay, $\tau_d = 0$, for different effective synaptic delays due to different synaptic rise times τ_1^I ($CV(I) = 0.05$, $I(I) = 15.8$ pA). For low τ_1^I (blue curve), the shift alternated in subsequent cycles reflecting the subharmonic nature of the rhythm. (E) The Fourier spectrum of the LFP as a function of the effective synaptic delay (synaptic time constant of rise τ_1^I). With decreasing τ_1^I , a subharmonic peak emerged and eventually the rhythm disintegrated. Parameters as in D. In (A), (B) and (D), perturbations were made with a square-wave inhibitory current pulse with duration 0.1 ms to each interneuron. In (A) and (B), the amplitude of the current was 1600 pA, resulting in a 2 mV rapid hyperpolarization. In (D), the amplitude of the current was 400 pA, resulting in a 0.5 mV rapid hyperpolarization.

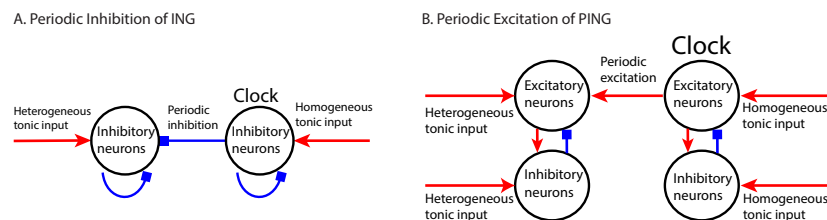


Figure 4: Sketch of computational models. (A) ING rhythm receives periodic inhibitory input generated from another ‘clock’ ING rhythm. (B) PING rhythm receives periodic excitatory input by its E-population generated from another ‘clock’ PING rhythm.

177 In [13, 27] the exact reduction of all-to-all coupled heterogeneous networks of quadratic integrate-fire
 178 neurons to 2 coupled ordinary differential equations for each network [23] has been used to obtain the
 179 infinitesimal macroscopic phase-response curve (imPRC) for ING and PING networks. They obtained
 180 biphasic response only if the excitatory perturbation was applied to the population of inhibitory
 181 neurons; for perturbations to the excitatory neurons they found only monophasic response (type-I).
 182 This is presumably due to the lack of a delay in the single-exponential synaptic interactions used
 183 in [13, 27].

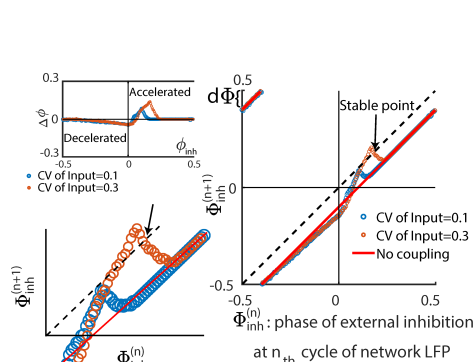
184 **Enhancing entrainment of ING-rhythms through network heterogeneity**

185 In order to allow communication by coherence [11, 32], the rhythms in different brain areas need to
 186 be sufficiently phase-locked with each other. As a simplification of two interacting γ -rhythms, we
 187 therefore investigated the ability of the rhythm in a network to be entrained by a periodic external
 188 input, particularly focusing on the possibly facilitating role of neuronal heterogeneity. Motivated by
 189 the paradoxical phase response induced by the heterogeneity, we addressed, in particular, the question
 190 whether an ING network can be sped up by inhibition to entrain it with a faster network.

191 The network considered here was the same as that used to analyze the fmPRC. The within-network
 192 interaction was an all-to-all inhibition with synaptic delay τ_d , resulting in a rhythm with natural
 193 frequency $f_{natural}$. Each neuron received heterogeneous input I_{bias} and inhibitory periodic pulses with
 194 frequency f_{clock} . The latter can be considered as the output of another ING-network and were,
 195 in fact, generated that way (Fig.4). We refer to this external input as the ‘clock’. The detuning
 196 $\Delta f = f_{clock} - f_{natural}$ was a key control parameter.

197 For periodic input the fmPRC allows the definition of an iterated map describing the response of the
 198 network. For periodic δ -pulses that map is shown in Fig.5A. For positive detuning, i.e. when the clock

A. Iterated Map



B. Period-Doubling Cascade and Chaos

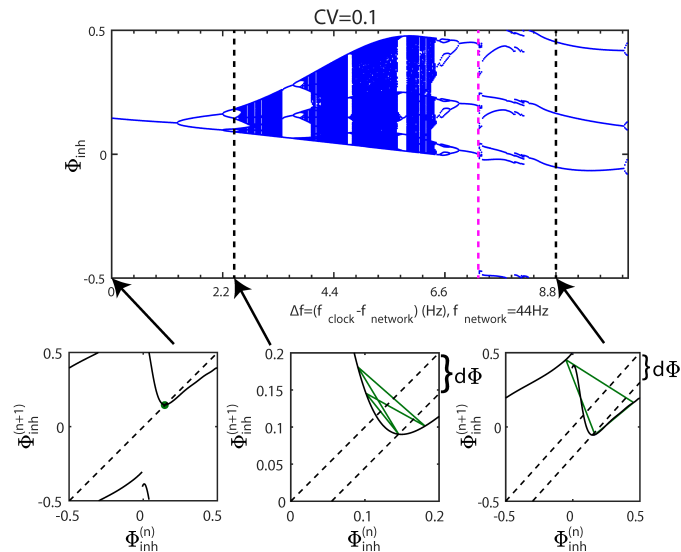


Figure 5: Connection between fmPRC and the synchronization of γ -rhythms. (A) Iterated map of Φ_{inh} . The network can be synchronized by faster periodic inhibition under sufficiently large advancing phase response. (B) Top: The bifurcation diagram of the iterated map of Φ_{inh} with varying detuning Δf . To the right of the magenta dashed line ($\Delta f = 7.28$ Hz) the attractors involve points on both sides of the discontinuity of the map. Bottom from left to right: iterated maps of Φ_{inh} for $\Delta f = 0, 2.44, 8.8$ Hz. The distance between the diagonal and subdiagonal line represents the detuning between the network and periodic input. In (A), the fmPRC was determined for a δ -pulse perturbation, in (B) for a double-exponential inhibitory current (cf. (2,3)) was used as in Fig.6.

199 is faster than the network, entrainment requires that the phase response is paradoxical in order for
 200 the rhythm to be sped up by the inhibition. If the heterogeneity and the resulting phase response are
 201 sufficiently large, the maximum of the iterated map crosses the diagonal, generating a stable and an
 202 unstable fixed point. The former is the desired entrained state.

203 As the detuning is increased the iterated map is shifted downward. This can decrease the slope of the
 204 iterated map at the fixed point below -1, destabilizing the fixed point in a period-doubling bifurcation.
 205 For periodic pulses comprised of double-exponential inhibitory currents (cf. (2,3)) a rich bifurcation
 206 scenario emerged (Fig.5B). Note that the full map is not continuous and not unimodal (cf. first bottom
 207 panel of Fig.5B). Nevertheless, for $\Delta f < 7.17$ Hz the attractor remains near the unstable fixed point
 208 and displays a period-doubling cascade to chaos and multiple periodic windows. For $\Delta f > 7.28$ Hz,
 209 however, the attractor includes points on both sides of the discontinuity (cf. third bottom panel in
 210 Fig.5B).

211 Having clarified the role of the fmPRC in the network's synchronizability and ability to phase-lock,

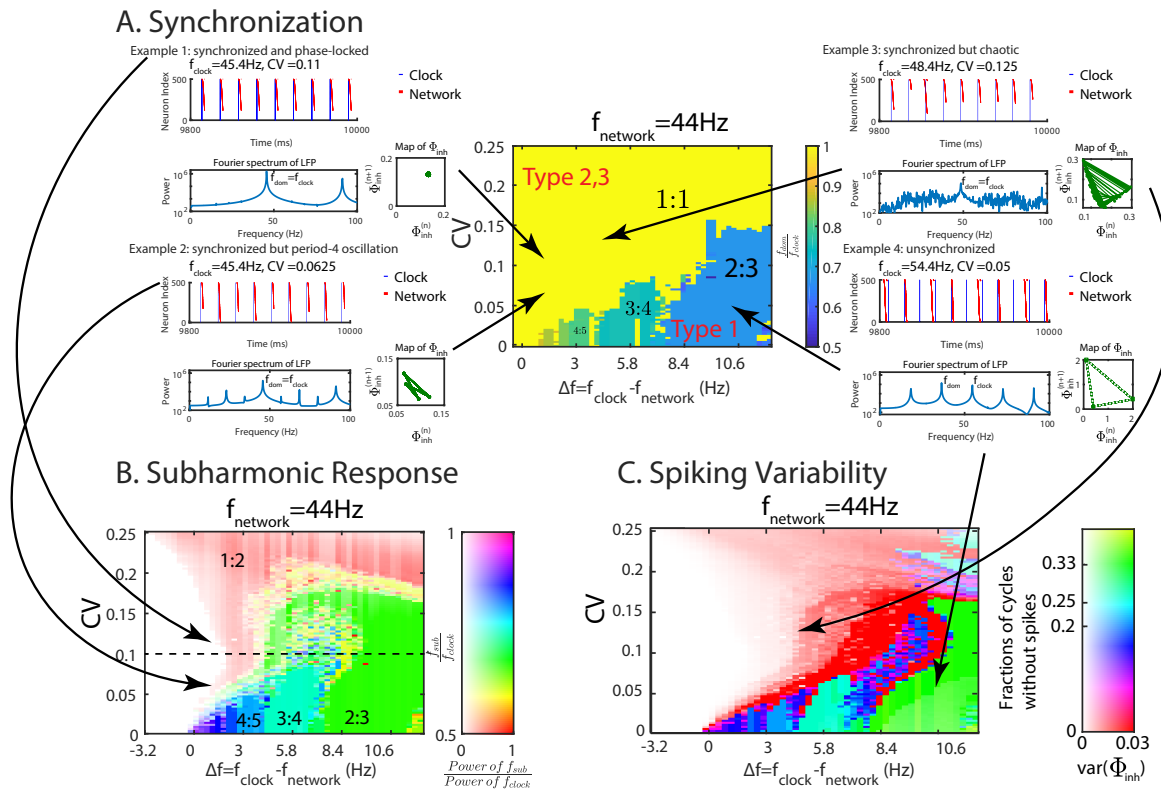


Figure 6: Network heterogeneity enhances synchronization and phase-locking of periodically driven ING rhythm. (A) Synchronization quantified using $f_{dom} : f_{clock}$ with f_{dom} and f_{clock} being the dominant frequencies of the Fourier spectrum of the LFP of the network and the clock, respectively. The neuronal heterogeneity enhanced the synchronization by shifting f_{dom} to f_{clock} . Example 1: Synchronized with 1:1 phase-locking. Example 2: Synchronized with subharmonic response (period 4). Example 3: synchronized with subharmonic response (chaotic). Example 4: Not synchronized. Squares and dashed lines in the map of Φ_{inh} indicate clock cycles in which the network did not spike (Φ_{inh} was arbitrarily set to 2). (B) Subharmonic response. Color hue and saturation indicate the frequency ratio $f_{sub} : f_{clock}$ and the ratio of the Fourier power at these two frequencies. f_{sub} is the frequency of the dominant peak of the network power spectrum that satisfies $f_{sub} < f_{clock}$. The power ratio is capped at 1. Dashed line marks the value of input heterogeneity used in Fig.5B. (C) Spiking variability and $var(\Phi_{inh})$ as a function of neuronal heterogeneity and detuning. Color hue indicates the fraction of clock cycles without spikes in the network. In particular, red indicates that the network spikes in every cycle. Color saturation indicates $var(\Phi_{inh})$. The neuronal heterogeneity enhances the tightness of the phase-locking.

212 we investigated the role of neuronal heterogeneity in more detail (Fig.6). To do that, we adjusted for
213 each value of the input heterogeneity the mean input strength $I^{(I)}$ so as to keep the natural frequency
214 $f_{network}$ constant ($f_{network} = 44$ Hz). Then we determined the extent of synchronization and phase-
215 locking of the network under the influence of periodic inhibitory input as a function of the detuning
216 Δf and network heterogeneity CV . As shown above, the fmPRC of a heterogeneous network could
217 be biphasic with the amplitude of the paradoxical phase response increasing with neuronal hetero-
218 geneity. Expecting that for sufficiently large heterogeneity an ING-rhythm could be accelerated by a
219 faster periodic inhibition, we tested phase-locking predominantly for positive detuning, corresponding
220 to $f_{clock} > f_{network}$. We first investigated how neuronal heterogeneity affected the synchronization by
221 comparing the dominant frequency f_{dom} in the Fourier spectrum of the network's LFP with f_{clock} . In
222 Fig.6A, the color hue indicates the ratio $f_{dom} : f_{clock}$. For small heterogeneity, f_{dom} was a rational
223 multiple of f_{clock} that depended on the detuning, while for sufficiently large CV the network became
224 synchronized in the sense that $f_{dom} = f_{clock}$ (yellow). The range of Δf allowing synchronization be-
225 came wider with increasing neuronal heterogeneity, implying that the neuronal heterogeneity enhanced
226 the synchronization of the ING-rhythm. However, note that $f_{dom} = f_{clock}$ did not imply a perfectly
227 synchronized or a 1:1 phase-locked state. In fact, various different subharmonic responses arose: ex-
228 ample 2 shows a period-4 state, while in example 3 the dynamics were actually chaotic (Fig.6A) even
229 though $f_{dom} = f_{clock}$. Motivated by these observations, we divided the states into three types:

- 230 • Type 1: $f_{dom} \neq f_{clock}$, not synchronized, not phase-locked (Fig.6 example 4).
- 231 • Type 2: $f_{dom} = f_{clock}$ with subharmonic response, might be poorly phase-locked (Fig.6 example
232 3) or displaying rational ratio phase-locking (Fig.6 example 2).
- 233 • Type 3: $f_{dom} = f_{clock}$, no subharmonic response, 1-to-1 phase-locking (Fig.6 example 1).

234 The phase diagram Fig.6A does not differentiate between types 2 and 3. It only shows that neuronal
235 heterogeneity enhanced the synchronization of the network by shifting f_{dom} to f_{clock} . Therefore, we
236 studied whether neuronal heterogeneity also enhanced the synchronization by weakening the subhar-
237 monic response and changing the synchronized state from type 2 to type 3, as well as whether the
238 dynamics of the fmPRC shown in the bifurcation diagram Fig.5B could predict the phase relationship
239 between the network and the clock. Using the same simulation setup as in Fig.6A, the subharmonic
240 response is shown in Fig.6B. The color hue indicates the ratio $f_{sub} : f_{clock}$, where f_{sub} is the frequency
241 of the dominant peak of the LFP power spectrum that satisfies $f_{sub} < f_{clock}$. The color saturation

242 gives the ratio of the powers at f_{sub} and f_{clock} (capped at 1). Thus, over most of the range of positive
243 detuning and neuronal heterogeneity tested, the fading-away of the color with increasing heterogeneity
244 reveals that the neuronal heterogeneity weakened the subharmonic response. Over a small range of
245 positive detuning, increasing neuronal heterogeneity from small values induced perfect synchronization
246 (type 3) by weakening the subharmonic response with frequency ratio $f_{sub} : f_{clock} = 1 : 2$; the system
247 traversed a continuous period-doubling bifurcation in reverse, with type 2 (red) giving way to type 3
248 (white). Together with Fig.6A, this showed that neuronal heterogeneity could enhance the synchro-
249 nization both by making $f_{dom} = f_{clock}$ (from type 1 to type 2) and by weakening the subharmonic
250 response (from type 2 to type 3). The range of detuning where increasing heterogeneity induced a
251 type 3 synchronization became wider for larger synaptic delay within the network (Suppl. Figure S3).
252 Note that the bifurcation diagram (Fig.5B) based on the fmPRC agrees well with the subharmonic
253 response marked along the dashed line at $CV = 0.1$ in Fig.6B, suggesting that the fmPRC can well
254 predict the subharmonic response and persistent phase response of the network.

255 In addition to enhancing the frequency synchronization, neuronal heterogeneity was also able to increase
256 the tightness of the phase-locking. Over most of the parameter regime investigated, the variance of the
257 phase of the network relative to the periodic input ($var(\Phi_{inh})$) decreased with increasing heterogeneity,
258 as indicated by the decrease in the color saturation in Fig.6C. In fact, for detuning between 0 Hz and
259 2 Hz the heterogeneity reduced $var(\Phi_{inh})$ to 0 (white), corresponding to the 1:1 phase-locked state.
260 Even for the 1:2 phase-locked state (cf. the red area in Fig.6B) $var(\Phi_{inh})$ was very small for a range
261 of heterogeneity and detuning (2 Hz to 4 Hz), indicating tight phase locking. Except for type-3
262 synchronized states the size of the spike volleys varied between clock cycles. In fact, over wide ranges
263 of the parameters the network did not spike in each of the clock cycles, as indicated by the color hue
264 in Fig.6C, which gives the fraction of cycles with no network spikes (e.g. Fig.6 example 4).

265 **Paradoxical phase response and entrainment of PING rhythms**

266 Many γ -rhythms involve not only inhibitory neurons, but arise from the mutual interaction of excitatory
267 (E) and inhibitory (I) neurons (PING rhythm) [33]. The key elements to obtain a paradoxical phase
268 response and the ensuing enhanced synchronization are self-inhibition within the network, neuronal
269 heterogeneity and effective synaptic delay. Since in PING rhythms the connections from E-cells to
270 I-cells and back to the E-cells form an effective self-inhibiting loop, we asked whether PING-rhythms
271 can exhibit behavior similar to the behavior we identified for ING-rhythms.

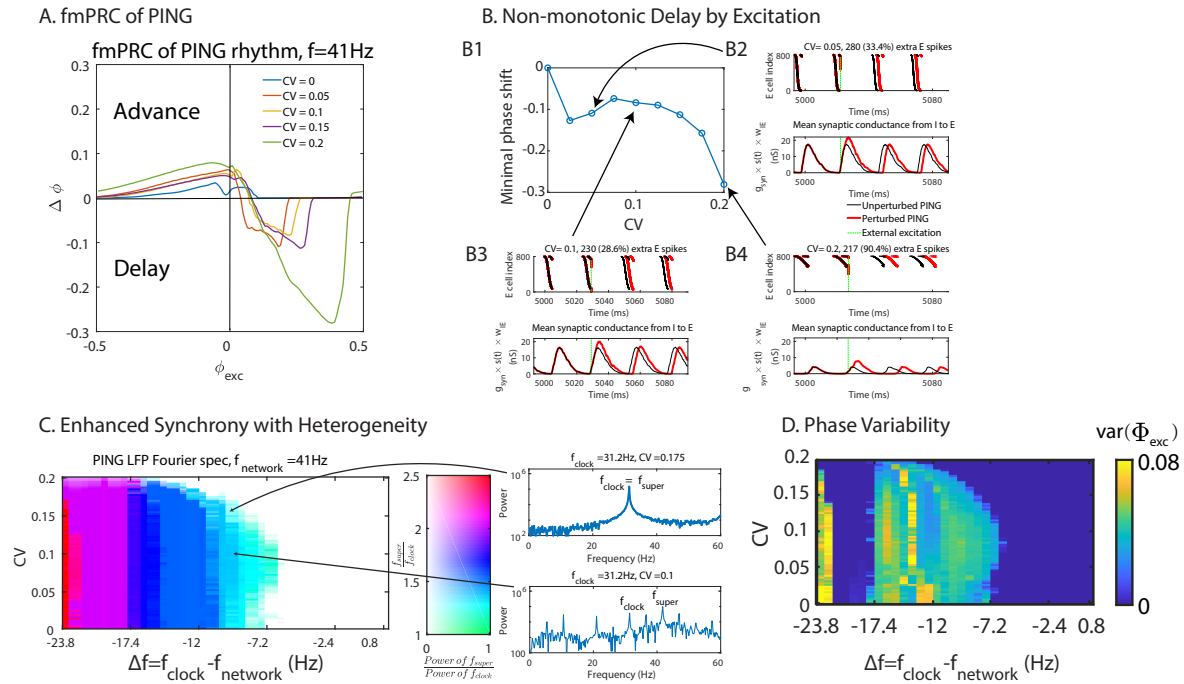


Figure 7: Network heterogeneity enhances the synchronization and the tightness of phase-locking of the PING rhythm. (A) fmPRC of PING networks with constant natural frequency ($f_{network} = 41$ Hz) but different neuronal heterogeneity. Only with neuronal heterogeneity the phase was delayed by the excitation. (B) Non-monotonicity of the paradoxical delay with constant natural frequency ($f_{network} = 41$ Hz). B2-4: Top: raster plot of spikes in E-population (input strength increased with cell index). Bottom: mean inhibitory synaptic conductance within the PING network. The titles show the absolute and relative increase in spike number (B2: $CV = 0.05$, B3: $CV = 0.1$, B4: $CV = 0.2$). (C) Subharmonic response of the PING rhythm with periodic excitation as function of neuronal heterogeneity and detuning. $f_{network}$ was fixed at 41 Hz. Color hue and saturation indicate the frequency ratio and power ratio at the frequencies f_{super} and f_{clock} of the E-population's LFP. f_{super} was the frequency of the dominant peak of the LFP power spectrum that satisfies $f_{super} > f_{clock}$. The power ratio was capped at 1. Generally, the neuronal heterogeneity enhanced the synchronization of the PING rhythm by weakening subharmonic response. (D) The tightness of the phase-locking ($var(\Phi_{exc})$) as a function of neuronal heterogeneity and detuning. The neuronal heterogeneity enhanced the tightness of the phase-locking. For $\Delta f \in [-22\text{Hz}, -17.4\text{Hz}]$ the clock was twice as fast as the network, resulting in vanishing $var(\Phi_{exc})$.

272 Considering a PING-rhythm generated by an E-I network comprised of integrate-fire neurons, we first
273 studied its fmPRC. To avoid that all I-cells receive identical input and therefore spike as a single unit,
274 the I-cells received, in addition to the excitation from the E-cells, heterogeneous, tonic, Gaussian-
275 distributed subthreshold input with mean $I^{(I)} = 36$ pA and $CV^{(I)} = 0.167$. The phase response of
276 the network was probed by applying an identical external excitatory perturbation to all E-cells and
277 recording the resulting phase shift of the LFP (cf. eqs.(7,8)) of the E-population, averaged across
278 500 realizations of the subthreshold input to the I-cells (Fig.7A). More specifically, the perturbations
279 consisted of a square-wave excitatory current pulse with amplitude 76 pA and duration 0.1 ms to each
280 E-cell, resulting in a 2 mV rapid depolarization. Without neuronal heterogeneity the external excitation
281 always advanced the phase of the rhythm resulting in an fmPRC that was strictly positive. In the
282 heterogeneous case, however, the PING rhythm exhibited a paradoxical phase response, whereby the
283 collective rhythm was delayed while the individual neurons were advanced by the excitation. The delay
284 was caused by the increase of self-inhibition within the network that was generated by the additional
285 spikes in the E-population, which in turn drove additional spikes in the I-population. In contrast to the
286 fmPRC of the ING-rhythm, this paradoxical phase response was not monotonic in the heterogeneity.
287 While weak heterogeneity resulted in strong delay, the delay decreased with increasing intermediate
288 CV-values and only increased again for larger CV (Fig.7B left top). This non-monotonicity arose
289 because we kept the frequency of the network constant as we increased its heterogeneity. This required
290 a decrease in the tonic input to the E-cells with increasing heterogeneity. For the stronger tonic input
291 used for weak heterogeneity the same external perturbation elicited more additional spikes than it did
292 for strong heterogeneity where the tonic input was weaker (cf. titles of subpanels of Fig.7B). The total
293 number of spikes occurring in each cycle of the unperturbed network also decreased with increasing
294 heterogeneity. Consequently, the relative change in the number of spikes induced by the perturbation
295 was non-monotonic in the heterogeneity. As a result, the relative change in the inhibitory synaptic
296 conductance resulting from the perturbation and with it the phase delay was also non-monotonic.

297 As for the ING rhythm, we investigated the role of neuronal heterogeneity in the synchronizability and
298 the ability of phase-locking of coupled PING rhythms. In analogy to the ING-case, we considered
299 the case of the E-population of a PING network receiving periodic excitation generated by a clock
300 PING network (Fig.4B). As before, we adjusted the tonic input strength to the E-population to keep
301 the natural frequency of the network constant as we changed its heterogeneity ($f_{network} = 41$ Hz).
302 To probe the impact of the paradoxical phase response on the synchronization we focused on nega-

303 tive detuning for which the periodic external excitation needed to slow down the network in order to
304 achieve phase-locking. Indeed, with increasing heterogeneity the network could become synchronized
305 with the slower clock over a larger range of the detuning as indicated by the fading saturation of the
306 color in Fig.7C. Here the color hue indicates the ratio $f_{super} : f_{clock}$, where f_{super} was determined as
307 the frequency with the most power among the frequencies higher than f_{clock} in the Fourier spectrum
308 of the E-population's LFP. The color saturation indicates the ratio of the power at the frequencies
309 f_{super} and f_{clock} . Thus, a color hue closer to green ($f_{super} : f_{clock} = 1 : 1$) or with a lower saturation
310 implies better synchronization. By observing how the width of the range of detuning allowing
311 synchronization varied with neuronal heterogeneity, we concluded that generally, the synchronizability
312 of PING rhythm was enhanced by the neuronal heterogeneity by weakening subharmonic response.
313 Note that for $CV \in [0, 0.1]$ the synchronizability of the PING rhythm decreased slightly with neuronal
314 heterogeneity. This was consistent with the nonmonotonicity exhibited by the fmPRC seen in
315 Fig.7B. The neuronal heterogeneity played a similar role in the tightness of the phase-locking as in the
316 synchronizability (Fig.7D).

317 **3 Discussion**

318 In this paper we have analyzed the response of collective oscillations of inhibitory and of excitatory-
319 inhibitory networks of integrate-fire neurons to external perturbations. For ING- and PING-rhythms
320 we have shown that the combination of neuronal heterogeneity and effective synaptic delay can qualitatively
321 change the phase response compared to the phase response of the individual neurons generating
322 the rhythm. Thus, perturbations that delay the I-cells can paradoxically advance the ING-rhythm
323 and perturbations that advance the E-cells can delay the PING-rhythm. As a result, the macroscopic
324 phase-response curve for finite-amplitude perturbations (fmPRC) of the rhythm can change sign as the
325 phase of the perturbation is changed (type-II), even though the PRC of all individual cells is strictly
326 positive (type-I). This change of the fmPRC enhances the ability of the γ -rhythm to synchronize with
327 other rhythms.

328 The key element of the mechanism driving the paradoxical phase response and the enhanced synchrono-
329 zation is the cooperation of the external perturbation and the effectively delayed within-network
330 inhibition. In the ING-network a suitably timed external perturbation delays the lagging - but not
331 the early - neurons sufficiently to allow the within-network inhibition triggered by the early neurons

332 to keep the lagging neurons from spiking. This reduces the overall within-network inhibition and with
333 it the duration of the cycle. Thus, the perturbation modifies the internal dynamics of the rhythm,
334 which leads to changes in the phase of the rhythm that can dominate the immediate phase change the
335 perturbation induces. The situation is somewhat similar to that investigated in [18]. There it had been
336 pointed out that an external perturbation of a collective oscillation can lead to changes in its phase in
337 two stages: i) an immediate change of the phases of all oscillators as a direct result of the perturbation
338 and ii) a subsequent slower change in the collective phase resulting from the convergence of the dis-
339 turbed phases back to the synchronized state. That analysis was based on a network of phase oscillators
340 and could therefore not include a key element of our results, which is the perturbation-induced change
341 in the number of neurons that actually spike and the resulting change in the within-network inhibition
342 that results in a change of the period of the rhythm. As discussed in [31, 34], for ING-rhythms such a
343 change in the number of spiking neurons underlies also the enhanced phase-locking found in [30].
344 Going beyond ING-rhythms, we showed that PING-rhythms can also exhibit a paradoxical phase re-
345 sponse *via* a mechanism that is analogous to that of ING-rhythms. For that analysis we have focused
346 on excitatory-inhibitory networks with only connections between but not within the excitatory and
347 inhibitory populations. For excitatory inputs to the excitatory cells to generate a paradoxical phase
348 response it is necessary that the additional spikes of the excitatory neurons that are caused by the
349 external perturbation induce additional spikes of the inhibitory neurons. This behavior arises if the
350 inhibitory population is also allowed to be heterogeneous. Moreover, the within-network inhibition has
351 to be strong enough to be able to suppress the spiking of lagging excitatory neurons. This is, e.g., found
352 in mice piriform cortex, where principal neurons driven by sensory input from the olfactory bulb arriv-
353 ing early during a sniff recruit inhibitory interneurons via long-range recurrent connections, resulting
354 in the global, transient suppression of subsequent cortical activity [35]. A characteristic feature of the
355 paradoxical phase response of the PING rhythm is the extended cycle time following enhanced acti-
356 vation of the excitatory cells. A strong such correlation between the cycle time and the previous LFP
357 amplitude has been observed for the γ -rhythm in hippocampus [36]. To assess whether this rhythm
358 exhibits paradoxical phase response would require comparing the macroscopic phase response [37] with
359 that of individual participating neurons.

360 In order for the global perturbation to affect the various neurons differently, they have to be at different
361 phases in their cycle. Our analysis suggests that the specific cause for this heterogeneity in the spike
362 times does not play an important role. Indeed, as shown in [29], even fluctuating heterogeneities that

363 are generated by noise rather than static heterogeneities reflecting intrinsic properties of neurons can
364 enhance the synchronization of multiple γ -rhythms in interconnected networks of identical neurons.
365 Note that the noise driving this synchronization is uncorrelated across neurons. The analysis of that
366 system revealed the same mechanism at work as the one identified here.

367 In various previous analytical and computational analyses it has been found that the dynamics of the
368 macroscopic phase of a collective oscillation can qualitatively differ from that of the microscopic phase.
369 Thus, for interacting groups of noisy identical phase oscillators the macroscopic phases of the groups
370 can tend to lign up with each other, even if all pair-wise interactions between individual oscillators
371 prefer the antiphase state, and vice versa [20]. An analogous result has been obtained for heterogeneous
372 populations of noiseless oscillators [17].

373 Qualitative changes have also been found in the macroscopic phase response of rhythms in noisy
374 homogeneous networks when the noise level was changed [21, 22, 28]. Using a Fokker-Planck approach
375 for globally coupled excitable neurons, a type-I mPRC was obtained for weak noise, where the rhythm
376 emerges through a SNIC bifurcation, while a type-II mPRC arose for strong noise that led to a
377 Hopf bifurcation [21]. A similar approach was used to obtain the mPRC via the adjoint method for
378 an extension of the theta-model that implements conductance-based synaptic interactions. Again,
379 although individual theta-neurons have a type-I PRC, a type-II mPRC was obtained for the rhythm,
380 which arose in a Hopf bifurcation [22]. This was also the case in an extension to networks of excitable
381 and inhibitory neurons [28].

382 Thus, results reminiscent of those presented here have been obtained previously. However, the mech-
383 anism underlying them was not addressed in detail and remained poorly understood. We expect that
384 our analysis will provide insight into those systems. The key element of the mechanism discussed here
385 is that due to the dispersion of the spike times, which either results from neuronal heterogeneity or
386 noise, the external perturbation enables the within-network inhibition to suppress the spiking of a
387 larger number of neurons than without it. In our system this was facilitated by the delay with which
388 spikes triggered the within-network inhibition, which allowed some neurons to escape its impact in
389 the absence of the external perturbation, but not in its presence. Our analysis showed, however, that
390 the explicit delay is not necessary; the effective delay resulting from a double-exponential synaptic
391 interaction is sufficient. In fact, when reducing that effective delay the paradoxical phase response
392 did not disappear until the delay was so short that the rhythm itself developed a strong subharmonic
393 component and disintegrated.

394 In this paper we have focused on a specific, very simple neuronal model, the leaky integrate-fire model
395 with conductance-based pulsatile coupling. In previous work on the enhanced synchronization among
396 γ -rhythms *via* noise-induced spiking heterogeneity it was demonstrated that this result does not depend
397 sensitively on the neuron type. Comparable results were obtained also with Morris-Lecar neurons for
398 parameters in which the periodic spiking arises from a SNIC-bifurcation, resulting in a type-I PRC as
399 is the case for integrate-fire neurons, but also for parameters for which the spiking is due to a Hopf
400 bifurcation, resulting in a type-II PRC [29]. For networks comprised of heterogeneous neurons with
401 type-II PRC the fmPRC of the collective oscillation is likely to be more complex, since the heterogeneity
402 allows the same input to induce phase shifts with opposite signs for different neurons. However,
403 we expect that the interplay between the within-network inhibition and the external perturbation
404 can again substantially and qualitatively modify the fmPRC by changing the number of neurons
405 participating in the rhythm.

406 In [29] the results were also found to be robust with respect to significant changes in the network
407 connectivity (random instead of all-to-all) as well as the reversal potential of the inhibitory synapses,
408 as long as the rhythm itself persisted robustly (cf. [38]). In fact, the coupling did not even have to
409 be synaptic; collective oscillations of relaxation-type chemical oscillators that were coupled diffusively
410 were also shown to exhibit noise-induced synchronization. These results suggest that the paradoxical
411 phase response found here arises in a much wider class of macroscopic collective oscillations.

412 The strong paradoxical phase response that we demonstrated for heterogeneous networks allows their
413 rhythm to synchronize with a periodic external input over a range of detuning that increases sub-
414 stantially with the neuronal heterogeneity. This is reminiscent of computational results for anterior
415 cingulate cortex that investigated networks of excitatory neurons coupled via a common population
416 of inhibitory neurons. There heterogeneity was also found to enhance the synchrony of rhythms, as
417 measured in terms of coincident spikes within 10ms bins [39].

418 The heterogeneity-enhanced synchrony we have identified suggests that the coherence of γ -rhythms
419 emerging in different interacting networks could also be enhanced by neuronal heterogeneity. It has
420 been proposed that the coherence of different γ -rhythms, which has been observed to be modified
421 by attention [8], plays an important role in the communication between the corresponding networks
422 [11,32]. Computational studies have shown that the direction of information transfer between networks
423 depends on the relative phase of their rhythms [12,13], which can be changed by switching between
424 different base states [40,41]. Whether the enhanced synchrony resulting from neuronal heterogeneity

425 enhances this information transfer is still an open question.

426 Disrupted γ -rhythms have been observed in multiple brain regions in neurological diseases, especially
427 Alzheimer’s disease. Optogenetic and sensory periodic stimulation at γ -frequencies has been found to
428 entrain the γ -rhythm in hippocampus and visual cortex, respectively, and has resulted in a significant
429 reduction in total amyloid level [42]. Similar neuro-protective effects of entrainment by external γ -
430 stimulation have also been found for other sensory modalities [14,43]. This suggests that γ -stimulation
431 by sensory input might be a feasible therapeutic approach. Our results suggest a potential role of
432 neuronal heterogeneity in this context.

433 From a functional perspective, it has been shown that the noise-induced synchronization mentioned
434 above can facilitate certain learning processes [44]. Specifically, a read-out neuron was considered
435 that received input from neurons in two networks *via* synapses that exhibited spike-timing dependent
436 plasticity. The two networks were interacting with each other and each of them exhibited a γ -rhythm,
437 albeit at different frequencies. For low noise the two rhythms were not synchronized and the read-out
438 neuron received inputs from the two networks at uncorrelated times. These inputs drove the plasticity
439 inconsistently, leading only to a very slow overall evolution of the synaptic weights, if any. However, for
440 stronger noise the two networks were synchronized, providing a more consistent spike timing that lead
441 to substantial changes in the synaptic weights. As a result, the read-out neuron was eventually only
442 driven by the network that had the larger natural frequency in the absence of the coupling between
443 the networks. It is expected that synchrony by neuronal heterogeneity will have a similar impact.

444 4 Methods

445 **Neuron model.** Both E-cells and I-cells were modeled as leaky integrate-and-fire neurons, each
446 characterized by a membrane potential $V_i(t)$ satisfying

$$\tau_{E,I} \frac{d}{dt} V_i = -(V_i - V_{rest}) + \frac{I_i^{(syn)}}{g_{syn}} + \frac{I_i^{(ext)}}{g_{ext}} + \frac{I_i^{(bias)}}{g_{bias}}, \quad (1)$$

447 where V_{rest} is the resting potential and $\tau_{E,I}$ the membrane time constants of the E- and I-cells,
448 respectively. $I_i^{(syn)}(t)$ is the total synaptic current that the neuron receives from the other neurons
449 within the network. $I_i^{(ext)}(t)$ is a time-dependent external input that represents perturbations applied
450 to determine the fmPRC or, in the study of synchronization, the periodic input generated by the

451 clock network. $I_i^{(bias)}$ denotes a tonic, neuron-specific excitatory bias current that implements the
 452 heterogeneity of the neuron properties. The corresponding conductances are denoted g_{syn} , g_{ext} , and
 453 g_{bias} . Upon the i^{th} neuron reaching the spiking threshold V_{peak} , the voltage V_i was reset to the fixed
 454 value V_{reset} . Parameters for the neuron were kept fixed throughout all simulations (see Table 1). The
 455 local field potential (LFP) of the network was approximated as the mean voltage across all neurons
 456 $j = 1, \dots, N$ in the respective population.

457 **Network model.** We studied two types of networks: an ING network and a PING network. The
 458 ING network was modeled as an all-to-all inhibitory network of $N_I^{(ING)}$ interneurons. The PING
 459 network was modeled as a network of $N_I^{(PING)}$ interneurons and $N_E^{(PING)}$ principal cells with all-to-
 460 all interneuron-principal and principal-interneuron connections (i.e., without principal-principal and
 461 interneuron-interneuron connections). In PING, only principal cells received external input $I^{ext}(t)$.

462 To gain insight into the interaction between two ING rhythms, we considered the simplified situation in
 463 which all neurons in the network received strictly periodic input $I^{(ext)}$, which was generated by another
 464 ING network ('clock'). Similarly, for PING rhythms, the E-cells of the PING network received strictly
 465 periodic excitatory input $I^{(ext)}$ from another PING network through all-to-all connection between their
 466 E populations.

467 **Synaptic currents.** We used delayed double-exponential conductance-based currents to model the
 468 excitatory and the inhibitory synaptic inputs from neuron j to neuron i ,

$$I_{ij}^{(syn)}(t) = g_{syn} \frac{\tau_{E,I}}{\tau_2^{E,I} - \tau_1^{E,I}} \left(A_{ij}^{(2)}(t) - A_{ij}^{(1)}(t) \right) (V_{rev,j} - V_i(t)), \quad (2)$$

469 with the two exponentials $A_{ij}^{(1,2)}(t)$ satisfying

$$\frac{d}{dt} A_{ij}^{(1,2)}(t) = -\frac{A_{ij}^{(1,2)}(t)}{\tau_{1,2}^{E,I}} + \sum_k W_{ij} \delta(t - t_j^{(k)} - \tau_d), \quad (3)$$

470 where $V_{rev,j}$ is the synaptic reversal potential corresponding to the synapse type, W_{ij} the dimensionless
 471 synaptic strength, and δ the Dirac δ -function. All synapses of the same type (I-I, I-E, E-I) were equally
 472 strong. The time constants of $A_i^{(1,2)}(t)$ satisfied $\tau_2^{E,I} > \tau_1^{E,I}$. The synaptic current was normalized
 473 to render the time integral independent of the synaptic time constants $\tau_{1,2}^{E,I}$. The inhibitory synaptic
 474 currents had a slower decay than the excitatory ones (cf. Table 1). We included an explicit synaptic
 475 delay τ_d in the model. Every spike of the presynaptic neuron j at time $t_j^{(k)}$ triggered a jump in both

476 $A_{ij}^{(1,2)}(t)$, making the synaptic conductance rise continuously after a synaptic delay τ_d .

477 External periodic inputs were also modeled as double-exponential conductance-based currents with
 478 g_{syn} in (2,3) replaced by g_{ext} . The time constants and delay were as for the within-network synaptic
 479 inputs.

480 **Heterogeneous tonic input.** The bias currents $I_i^{(bias)}$ of the ING network were Gaussian distributed
 481 around I_{mean} with a coefficient of variation CV and arranged in increasing order, $I_1^{(bias)} > I_2^{(bias)} \dots >$
 482 $I_N^{(bias)}$. For the PING network, all excitatory neurons received a heterogeneous bias $I_E^{(bias)}$ with mean
 483 $I^{(E)}$ and a coefficient of variation $CV^{(E)}$. Similarly, the bias currents $I_I^{(bias)}$ to the inhibitory neurons
 484 were characterized by their mean $I^{(I)}$ and their coefficient of variation $CV^{(I)}$. Without the excitatory
 485 input from principal cells, the voltage of interneurons remained below the spiking threshold. In our
 486 investigation of the impact of the neuronal heterogeneity on the phase response and entrainment of
 487 the PING rhythm we kept $CV^{(I)}$ fixed and varied $CV^{(E)}$.

488 **Macroscopic Phase-response Curve for Finite-Amplitude Perturbations (fmPRC).**

489 **ING rhythm.** For a single ING network, we applied a single inhibitory δ -pulse to each neuron
 490 $j = 1, \dots, N_I^{(ING)}$ at time t_{inh} (dashed green line in Fig.1B) and recorded the resulting phase shift $\Delta\phi$.
 491 The amplitude of the inhibitory perturbation to each neuron was the same. The phase of the inhibition
 492 was defined as

$$\phi_{inh} = \frac{t_{inh} - t_{firstspike}^{(unperturbed)}}{T}, \quad (4)$$

493 where T was the period of the network LFP and $t_{firstspike}^{(unperturbed)}$ the time of the first spike in the spike
 494 volley of the unperturbed network that was closest to t_{inh} . The resulting phase shift $\Delta\phi$ was given by

$$\Delta\phi = \frac{\left(t_{firstspike}^{(unperturbed)} - t_{firstspike}^{(perturbed)} \right)}{T}, \quad (5)$$

495 where $t_{firstspike}^{(perturbed)}$ is the time of the first spike in the corresponding volley in the perturbed network.
 496 $\Delta\phi$ and ϕ_{inh} were taken to be in the range $[-0.5, 0.5)$. Positive $\Delta\phi$ indicated that the network was
 497 advanced by the perturbation, while negative indicated a delay.

498 The periodic input ('clock') that was used to test the synchronizability of the ING-rhythm was gen-
 499 erated by a homogeneous ING network. The phase of the periodic input in the n^{th} clock cycle was
 500 defined by

$$\Phi_{inh}^{(n)} = \frac{\left(t_{firstspike}^{(clock)(n)} + \tau_d - t_{firstspike}^{(network)(n)}\right)}{T}, \quad (6)$$

501 where $t_{firstspike}^{(network)(n)}$ was the time of the first spike in the spike volley of the network in the n^{th} cycle and
 502 $t_{firstspike}^{(clock)(n)}$ the time of the spike of the clock. In contrast to the definition of ϕ_{inh} in (4), the definition
 503 of $\Phi_{inh}^{(n)}$ included the delay τ_d , since the inhibition generated by the clock arrived with delay τ_d in the
 504 network.

505 **PING rhythm.** To probe the phase response of the PING network we used the same approach as
 506 for the ING rhythm, except that we used excitatory instead of inhibitory δ -pulses and applied them
 507 only to the E-cells. The phase of the excitation ϕ_{exc} and the resulting phase shift $\Delta\phi$ were determined
 508 similarly as in the case of the ING rhythm,

$$\phi_{exc} = \frac{t_{exc} - t_{firstspike}^{(unperturbed)}}{T}, \quad (7)$$

$$\Delta\phi = \frac{\left(t_{firstspike}^{(unperturbed)} - t_{firstspike}^{(perturbed)}\right)}{T}, \quad (8)$$

509 where $t_{firstspike}^{(perturbed)}$ and $t_{firstspike}^{(unperturbed)}$ were the times of the first spike in the respective spike volleys of
 510 the E-population.

511 Analogously to $\Phi_{inh}^{(n)}$, the phase of the periodic input in the n^{th} clock cycle was given by

$$\Phi_{exc}^{(n)} = \frac{\left(t_{firstspike}^{(clock)(n)} + \tau_d - t_{firstspike}^{(network)(n)}\right)}{T}. \quad (9)$$

512 Throughout, the tonic, Gaussian distributed input to the interneurons in the PING network was fixed:
 513 $I^{(I)} = 36$ pA, $CV^{(I)} = 0.167$.

ING network

Parameter	Value
τ_I , membrane time constant	20 ms
u_{rest} , resting potential	-55 mV
V_{peak} , spiking threshold	-50 mV
V_{reset} , reset voltage	-60 mV
τ_d , synaptic delay	3 ms
$N_I^{(ING)}$, # of interneurons	500
W , synaptic strength within the network	7.5×10^{-3}
$W^{(ext)}$, synaptic strength for the input from the clock network	1.8×10^{-3}

PING network

Parameter	Value
τ_E , membrane time constant of principal cells	20 ms
τ_I , membrane time constant of interneurons	10 ms
u_{rest} , resting potential	-70 mV
V_{peak} , spiking threshold	-52 mV
V_{reset} , reset voltage	-59 mV
τ_d , synaptic delay	1 ms
$N_I^{(PING)}$, # of interneurons	200
$N_E^{(PING)}$, # of principal cells	800
W^I , inhibitory synaptic strength within the network	5.4×10^{-3}
W^E , excitatory synaptic strength within the network	1.67×10^{-3}
$W^{(ext)}$, clock-network synaptic strength	1.6×10^{-3}

Synaptic currents

Parameter	Value
τ_1^E , time constant of rise in excitatory synapse	0.5 ms
τ_2^E , time constant of decay in excitatory synapse	2 ms
τ_1^I , time constant of rise in inhibitory synapse	0.5 ms
τ_2^I , time constant of decay in inhibitory synapse	5 ms
V_{rev}^I , reversal potential of inhibitory synapse	-70 mV
V_{rev}^E , reversal potential of excitatory synapse	0 mV

Synaptic conductances

Parameter	Value
Excitatory input on principal cells : $g_{ext}^{(PING)}$, $g_{bias E}^{(PING)}$	0.19 nS
Excitatory input on interneurons: $g_{bias}^{(ING)}$, $g_{syn EtoI}^{(PING)}$, $g_{bias I}^{(PING)}$	0.3 nS
Inhibitory input on principal cells: $g_{syn ItoE}^{(PING)}$	2.5 nS
Inhibitory input on interneurons: $g_{ext}^{(ING)}$, $g_{syn}^{(ING)}$	4 nS

Table 1: **Parameters used in the model.** Most parameters are based on [29, 45].

514

515 References

- 516 [1] Bruesselbach H, Jones DC, Mangir MS, Minden M, Rogers JL. Self-organized coherence in fiber
517 laser arrays. *Optics Letters*. 2005;30(11):1339–1341. doi:10.1364/OL.30.001339.
- 518 [2] Wiesenfeld K, Colet P, Strogatz SH. Synchronization Transitions in a Disordered Josephson Series
519 Array. *Phys Rev Lett*. 1996;76(3):404–407.
- 520 [3] Liu C, Weaver DR, Strogatz SH, Reppert SM. Cellular Construction of a Circadian Clock: Period
521 Determination in the Suprachiasmatic Nuclei. *Cell*. 1997;91(6):855–860.

- 522 [4] Venzin OF, Oates AC. What are you synching about? Emerging complexity of
523 Notch signaling in the segmentation clock. *Developmental Biology*. 2020;460(1):40–54.
524 doi:10.1016/j.ydbio.2019.06.024.
- 525 [5] Wang XJ. Neurophysiological and Computational Principles of Cortical Rhythms in Cognition.
526 *Physiol Rev*. 2010;90(3):1195–1268.
- 527 [6] Börgers C, Epstein S, Kopell NJ. Background gamma rhythmicity and attention in cortical local
528 circuits: a computational study. *Proc Natl Acad Sci U S A*. 2005;102(19):7002–7007.
- 529 [7] Börgers C, Kopell NJ. Gamma oscillations and stimulus selection. *Neural Comput*.
530 2008;20(2):383–414.
- 531 [8] Bosman CA, Schoffelen JM, Brunet N, Oostenveld R, Bastos AM, Womelsdorf T, et al. Atten-
532 tional stimulus selection through selective synchronization between monkey visual areas. *Neuron*.
533 2012;75:875–888. doi:10.1016/j.neuron.2012.06.037.
- 534 [9] Roberts MJ, Lowet E, Brunet NM, Ter Wal M, Tiesinga P, Fries P, et al. Robust Gamma Coher-
535 ence between Macaque V1 and V2 by Dynamic Frequency Matching. *Neuron*. 2013;78(3):523–536.
536 doi:10.1016/j.neuron.2013.03.003.
- 537 [10] Buzsaki G, Schomburg EW. What does gamma coherence tell us about inter-regional neural
538 communication? *Nature Neuroscience*. 2015;18(4):484–489. doi:10.1038/nn.3952.
- 539 [11] Fries P. Rhythms for Cognition: Communication through Coherence. *Neuron*. 2015;88:220–235.
540 doi:10.1016/j.neuron.2015.09.034.
- 541 [12] Palmigiano A, Geisel T, Wolf F, Battaglia D. Flexible information routing by transient synchrony.
542 *Nature neuroscience*. 2017;20:1014–1022. doi:10.1038/nn.4569.
- 543 [13] Dumont G, Gutkin B. Macroscopic phase resetting-curves determine oscillatory coherence and
544 signal transfer in inter-coupled neural circuits. *PLoS Computational Biology*. 2019;15:e1007019.
545 doi:10.1371/journal.pcbi.1007019.
- 546 [14] Adaikkan C, Middleton SJ, Marco A, Pao PC, Mathys H, Kim DNW, et al. Gamma Entrainment
547 Binds Higher-Order Brain Regions and Offers Neuroprotection. *Neuron*. 2019;102:929–943.e8.
548 doi:10.1016/j.neuron.2019.04.011.

- 549 [15] Schultheiss NW, Butera RJ. Phase Response Curves in Neuroscience. Springer; 2012.
- 550 [16] Brown E, Moehlis J, Holmes P. On the Phase Reduction and Response Dynamics of Neural
551 Oscillator Populations. *Neural Comput.* 2004;16(4):673–715.
- 552 [17] Kawamura Y, Nakao H, Arai K, Kori H, Kuramoto Y. Phase synchronization between collective
553 rhythms of globally coupled oscillator groups: noiseless nonidentical case. *Chaos* (Woodbury,
554 NY). 2010;20:043110. doi:10.1063/1.3491346.
- 555 [18] Levnajic Z, Pikovsky A. Phase resetting of collective rhythm in ensembles of oscillators.
556 *Physical review E, Statistical, nonlinear, and soft matter physics.* 2010;82:056202.
557 doi:10.1103/PhysRevE.82.056202.
- 558 [19] Kawamura Y, Nakao H, Arai K, Kori H, Kuramoto Y. Collective Phase Sensitivity. *Phys Rev*
559 *Lett.* 2008;101(2):024101.
- 560 [20] Kawamura Y, Nakao H, Arai K, Kori H, Kuramoto Y. Phase Synchronization Between Collective
561 Rhythms of Globally Coupled Oscillator Groups: Noisy Identical Case. *Chaos.* 2010;20(4):043109.
- 562 [21] Kawamura Y, Nakao H, Kuramoto Y. Collective phase description of globally coupled excitable
563 elements. *Physical review E, Statistical, nonlinear, and soft matter physics.* 2011;84:046211.
564 doi:10.1103/PhysRevE.84.046211.
- 565 [22] Kotani K, Yamaguchi I, Yoshida L, Jimbo Y, Ermentrout GB. Population dynamics of the
566 modified theta model: macroscopic phase reduction and bifurcation analysis link microscopic
567 neuronal interactions to macroscopic gamma oscillation. *J R Soc Interface.* 2014;11(95):20140058.
568 doi:10.1098/rsif.2014.0058.
- 569 [23] Montbrio E, Pazo D, Roxin A. Macroscopic description for networks of spiking neurons. *Physical*
570 *Review X.* 2015;5:021028.
- 571 [24] Ott E, Antonsen TM. Low dimensional behavior of large systems of globally coupled oscillators.
572 *Chaos.* 2008;18(3):037113. doi:10.1063/1.2930766.
- 573 [25] Luke TB, Barreto E, So P. Complete Classification of the Macroscopic Behavior of a
574 Heterogeneous Network of Theta Neurons. *Neural Computation.* 2013;25(12):3207–3234.
575 doi:10.1162/NECO_a.00525.

- 576 [26] Hannay KM, Booth V, Forger DB. Collective phase response curves for heterogeneous coupled
577 oscillators. *Physical Review E*. 2015;92(2):022923. doi:10.1103/PhysRevE.92.022923.
- 578 [27] Dumont G, Ermentrout GB, Gutkin B. Macroscopic phase-resetting curves for spiking neural
579 networks. *Physical Review E*. 2017;96:042311. doi:10.1103/PhysRevE.96.042311.
- 580 [28] Akao A, Ogawa Y, Jimbo Y, Ermentrout GB, Kotani K. Relationship between the mechanisms
581 of gamma rhythm generation and the magnitude of the macroscopic phase response function in
582 a population of excitatory and inhibitory modified quadratic integrate-and-fire neurons. *Physical*
583 *Review E*. 2018;97(1):012209. doi:10.1103/PhysRevE.97.012209.
- 584 [29] Meng JH, Riecke H. Synchronization by uncorrelated noise: interacting rhythms in interconnected
585 oscillator networks. *Scientific reports*. 2018;8:6949. doi:10.1038/s41598-018-24670-y.
- 586 [30] White JA, Banks MI, Pearce RA, Kopell NJ. Networks of interneurons with fast and slow
587 gamma-aminobutyric acid type A (GABA(A)) kinetics provide substrate for mixed gamma-theta
588 rhythm. *Proceedings of the National Academy of Sciences of the United States of America*.
589 2000;97(14):8128–8133. doi:10.1073/pnas.100124097.
- 590 [31] Sereney AK, Kopell NJ. Effects of Heterogeneous Periodic Forcing on Inhibitory Networks. *Siam*
591 *Journal on Applied Dynamical Systems*. 2013;12(3):1649–1684. doi:10.1137/12089274X.
- 592 [32] Fries P. A Mechanism for Cognitive Dynamics: Neuronal Communication Through Neuronal
593 Coherence. *Trends Cogn Sci*. 2005;9(10):474–480.
- 594 [33] Bartos M, Vida I, Jonas P. Synaptic mechanisms of synchronized gamma oscillations in inhibitory
595 interneuron networks. *Nature Reviews Neuroscience*. 2007;8(1):45–56. doi:10.1038/nrn2044.
- 596 [34] Cannon J, McCarthy MM, Lee S, Lee J, Börgers C, Whittington MA, et al. Neurosystems:
597 brain rhythms and cognitive processing. *The European journal of neuroscience*. 2014;39:705–719.
598 doi:10.1111/ejn.12453.
- 599 [35] Bolding KA, Franks KM. Recurrent cortical circuits implement concentration-invariant odor
600 coding. *Science (New York, NY)*. 2018;361. doi:10.1126/science.aat6904.
- 601 [36] Atallah BV, Scanziani M. Instantaneous Modulation of Gamma Oscillation Frequency by Balanc-
602 ing Excitation with Inhibition. *Neuron*. 2009;62(4):566–577. doi:10.1016/j.neuron.2009.04.027.

- 603 [37] Akam T, Oren I, Mantoan L, Ferenczi E, Kullmann DM. Oscillatory dynamics in the hip-
604 pocampus support dentate gyrus-CA3 coupling. *Nature Neuroscience*. 2012;15(5):763–768.
605 doi:10.1038/nn.3081.
- 606 [38] Börgers C, Krupa M, Gielen S. The Response of a Classical Hodgkin-Huxley Neuron To an
607 Inhibitory Input Pulse. *J Comput Neurosci*. 2010;28(3):509–526.
- 608 [39] Adams NE, Sherfey JS, Kopell NJ, Whittington MA, LeBeau FEN. Heterogeneity in Neu-
609 ronal Intrinsic Properties: A Possible Mechanism for Hub-Like Properties of the Rat An-
610 terior Cingulate Cortex during Network Activity. *Eneuro*. 2017;4(1):UNSP e0313–16.2017.
611 doi:10.1523/ENEURO.0313-16.2017.
- 612 [40] Witt A, Palmigiano A, Neef A, El Hady A, Wolf F, Battaglia D. Controlling the oscillation phase
613 through precisely timed closed-loop optogenetic stimulation: a computational study. *Front Neural*
614 *Circuits*. 2013;7:49. doi:10.3389/fncir.2013.00049.
- 615 [41] Kirst C, Timme M, Battaglia D. Dynamic information routing in complex networks. *Nature*
616 *Communications*. 2016;7:11061. doi:10.1038/ncomms11061.
- 617 [42] Iaccarino HF, Singer AC, Martorell AJ, Rudenko A, Gao F, Gillingham TZ, et al. Gamma fre-
618 quency entrainment attenuates amyloid load and modifies microglia. *Nature*. 2016;540(7632):230–
619 +. doi:10.1038/nature20587.
- 620 [43] Martorell AJ, Paulson AL, Suk HJ, Abdurrob F, Drummond GT, Guan W, et al. Multi-sensory
621 Gamma Stimulation Ameliorates Alzheimer’s-Associated Pathology and Improves Cognition. *Cell*.
622 2019;177:256–271.e22. doi:10.1016/j.cell.2019.02.014.
- 623 [44] Meng JH, Riecke H. Synchronization by uncorrelated noise: interacting rhythms in interconnected
624 neuronal networks. *BMC Neuroscience*. 2018;19 (Suppl 2):116.
- 625 [45] Brunel N, Wang XJ. What Determines the Frequency of Fast Network Oscillations With Irregular
626 Neural Discharges? I. Synaptic Dynamics and Excitation-Inhibition Balance. *J Neurophysiol*.
627 2003;90(1):415–430.

628 **Supplementary Information**

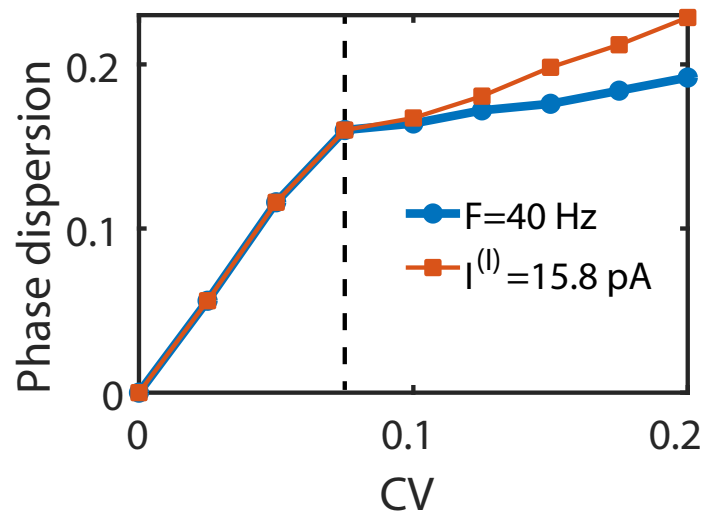


Figure S1: Dependence of the phase dispersion on the heterogeneity of the bias current. The phase dispersion was determined as the time difference between the first and the last spike in the same spike volley normalized by the period. Blue: fixed natural frequency ($f_{network} = 40\text{Hz}$) for different neuronal heterogeneity. Red: fixed mean input strength ($I^{(I)} = 15.8$ pA) for different neuronal heterogeneity. For $CV \geq 0.075$ (dashed line), some neurons spike more than once in a cycle.

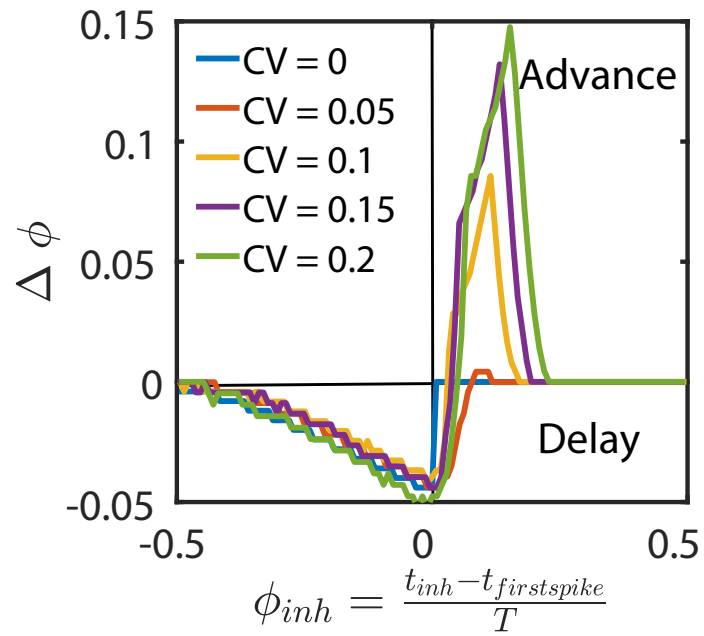


Figure S2: fmPRC of heterogeneous ING networks for fixed steady current ($I^{(I)} = 15.8$ pA) instead of fixed frequency (cf. Fig.2A). The paradoxical phase advance increased with neuronal heterogeneity.

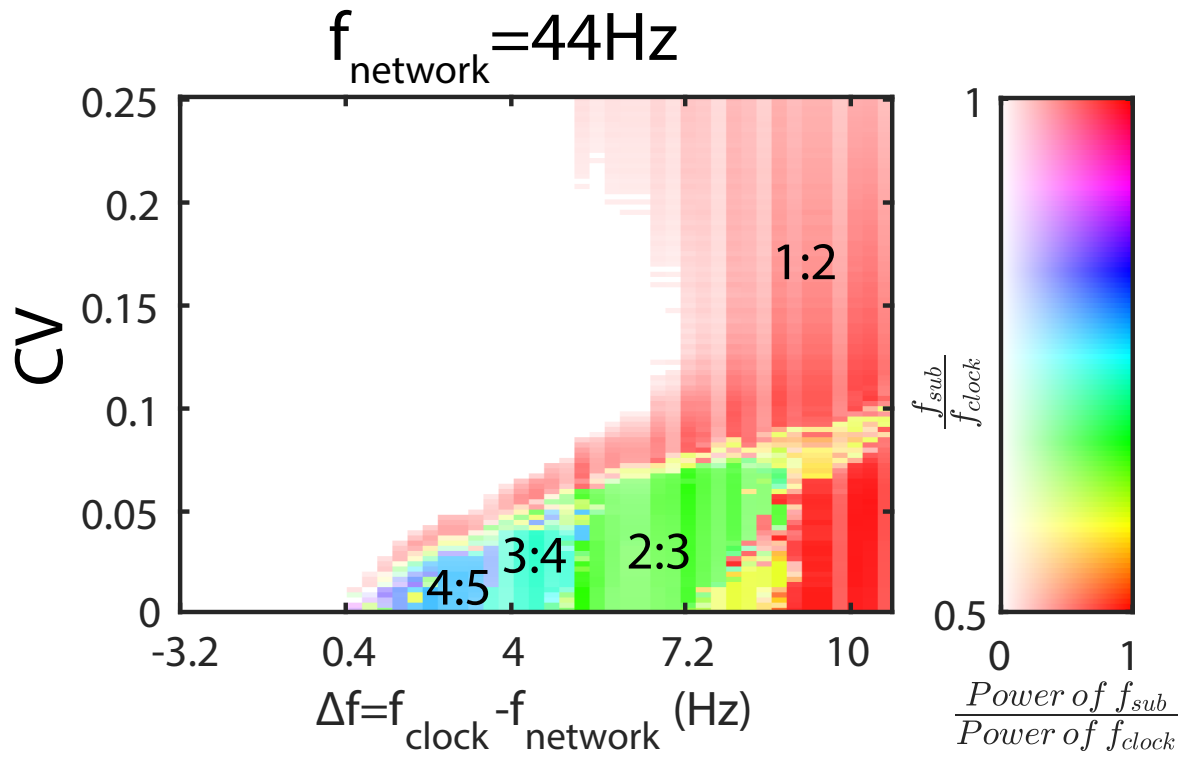


Figure S3: Subharmonic response of the ING rhythm with a longer synaptic delay within the network ($\tau_d = 5 \text{ ms}$) receiving periodic inhibitory input. For each value of the input heterogeneity, the natural frequency f_{network} was kept constant ($f_{\text{network}} = 44 \text{ Hz}$) by adjusting the mean input strength $I^{(I)}$. The range of detuning where increasing heterogeneity induced a type 3 synchronization became wider compared to Fig.6B, where $\tau_d = 3 \text{ ms}$. $W^{(ext)} = 1.2 \times 10^{-3}$.